QUANTAL EFFECTS ON GROWTH OF INSTABILITIES IN NUCLEAR MATTER

A THESIS SUBMITTED TO
THE GRADUATE SCHOOL OF NATURAL AND APPLIED SCIENCES
OF
THE MIDDLE EAST TECHNICAL UNIVERSITY

BY

DİLAN KAYA

IN PARTIAL FULFILLMENT OF THE REQUIREMENTS FOR THE DEGREE
OF
MASTER OF SCIENCE
IN
THE DEPARTMENT OF PHYSICS

JANUARY 2004

Approval of the Graduate School of Natural and Applied Sciences

Prof. Dr. Canan Özgen
Director

I certify that this thesis satisfies all the requirements as a thesis for the degree of Master of Science

Prof. Dr. Sinan Bilikmen
Head of Department

This is to certify that we have read this thesis and that in our opinion it is fully adequate, in scope and quality, as a thesis for the degree of Master of Science.

Prof. Dr. Şakir Ayık	Prof. Dr. Ahmet Gökalp
Co-Supervisor	Supervisor

Examining Committee Members

Prof. Dr. Mehmet Abak _____

Prof. Dr. Cüneyt Can _____

Prof. Dr. Ahmet Gökalp _____

Assoc. Prof. Dr. Gürsevil Turan _____

Prof. Dr. Osman Yılmaz _____

ABSTRACT

QUANTAL EFFECTS ON GROWTH OF INSTABILITIES IN NUCLEAR MATTER

Kaya, Dilan

M.S., Department of Physics

Supervisor: Prof. Dr. Ahmet Gökalp

Co-Supervisor: Prof. Dr. Şakir Ayık

January 2004, 41 pages

The quantal Boltzmann–Langevin equation is used to obtain a dispersion relation for the growth rates of instabilities in infinite nuclear matter. The dispersion relation is solved numerically for three different potentials. The quantal results are compared with the semi-classical solutions. It is seen that with the inclusion of the quantal effects the growth rates of the fastest growing modes in the system are reduced and these modes have the tendency to occur at longer wavelengths for all the potentials considered. Furthermore, the boundaries of the spinodal region is determined by the phase diagrams using the same three potentials and it is observed that the expanding nuclear matter undergoes liquid-gas phase transition at reduced temperatures when the quantum effects are included.

Keywords: Dispersion Relation, Spinodal Region.

ÖZ

NÜKLEER MADDE İÇİ KARARSIZLIKLARIN OLUŞUMUNDA KUANTAL ETKİLER

Kaya, Dilan

M.S., Department of Physics

Tez Yöneticisi: Prof. Dr. Ahmet Gökalp

Ortak Tez Yöneticisi: Prof. Dr. Şakir Ayık

Ocak 2004, 41 sayfa

Sonsuz nükleer madde içindeki kararsızlıkların oluşum oranı için bir dağılım bağıntısı elde etmek üzere kuantal Boltzmann–Langevin denklemi kullanıldı. Dağılım bağıntısı üç farklı potansiyel için nümerik olarak çözüldü. Kuantal sonuçlar yarı-klasik çözümlerle karşılaştırıldı. Uygulanan bütün potansiyeller için kuantal etkilerin dahil edilmesiyle sistemdeki en hızlı gelişen modların oluşum oranlarının azaldığı ve bu modların daha uzun dalga boylarında bulunma eğilimine sahip olduğu görüldü. Aynı üç potansiyel için faz dönüşüm bölgesinin sınırları faz diyagramları yardımıyla belirlendi ve kuantal etkilerin dahil edilmesiyle genişleyen nükleer maddenin sıvı-gaz faz dönüşümüne daha düşük sıcaklıklarda ulaştığı gözlendi.

Anahtar Kelimeler: Dağılım Bağıntısı, Faz Dönüşüm Bölgesi.

Dedicated to my sister, Berivan...

ACKNOWLEDGEMENTS

I would like to express my deepest gratitude and appreciation to my supervisor Prof. Dr. Ahmet Gökalp for his continuous support, guidance and understanding during the preparation of this thesis.

Nor can I forget what I owe Prof. Dr. Osman Yılmaz, who has made countless productive and useful suggestions in every part of this work.

Also I would like to appreciate Prof. Dr. Şakir Ayık who has made useful suggestions by devoting his valuable time to this work, which has greatly benefited from his careful reading and critical comments.

Special thanks to my mother, my father, my sister Berivan and my brother Cevdet for their love, support and understanding at all stages of my life.

Finally, I wish to thank the most important person in my life, Fatih M. Kavruk. The completion of this study would not have been possible without his endless love and faith in me.

TABLE OF CONTENTS

LIST OF FIGURES

FIGURES

CHAPTER 1

INTRODUCTION

Nuclear collisions provide opportunities to study the nuclear systems far from equilibrium. Due to the collisions, the nuclear system may develop into widely different configurations. The spinodal (volume) instabilities may appear and decomposition of the system may take place. The boundary that the system changes phase is called the spinodal boundary. In recent years, the feasibility of making detailed experimental studies at intermediate energies aroused the theoretical interest in developing the formal treatment of nuclear dynamics like the density fluctuations and spinodal instabilities.

The investigation of the decay properties of very hot nuclei is currently one of the most challenging topics of nuclear physics. The excitation energy of the hot nuclei is comparable with the total binding energy. They disintegrate via a new multi-body decay mode, thermal multifragmentation, which is characterized by the copious emission of intermediate mass fragments ($2<Z\leq20$). The development of this field has been strongly stimulated by the idea that this process is related to the liquid-gas phase transition, which was predicted on the basis of the similarity between van der Waals and nucleon-nucleon interactions. For both systems there is

a spinodal region characterized by phase instability. The density here is reduced as compared to the liquid phase. One can imagine that a hot nucleus at temperatures about T = 5-7 MeV expands due to thermal pressure and enters the unstable region. Due to density fluctuations, a homogeneous system converts into a mixed phase state consisting of droplets surrounded by nuclear gas. The final state of this transition is a nuclear fog, which explodes due to Coulomb repulsion and is detected as multifragmentation. The disintegration time is very short. This is the scenario of spinodal decomposition. It was proven experimentally that thermal multifragmentation occurs at reduced densities, and the disintegration time is less than 100 fm/c. The spinodal decomposition is, in fact, the liquid-fog phase transition in a nuclear system [1].

The decay of highly excited nuclear systems through a simultaneous disassembly into fragments and particles, what we call multifragmentation, is a subject of great interest. The process of multifragmentation following the collision of heavy nuclei in the region of medium energies displays several features analogous to usual liquid-gas phase transitions of water. However, in this analogy one should be aware of differences due to nucleon-nucleon interactions, finite size and quantum effects as well as binary, i.e. two-component, character of nuclear matter. Indeed after a fast compression and expansion we expect the system to be quenched into an unstable state either inside the coexistence curve in the metastability region where the phase is unstable against short wavelength but large amplitude of fluctuations, which means small sizes of nucleon groups or in the instability (spinodal) region where the system becomes unstable against long

wavelength but small amplitude fluctuations, that results in larger sizes of fragments. Then the system will evolve toward a stable thermodynamical state of two coexisting phases either through nucleation in the former case or through spinodal decomposition in the latter case [2, 3].

A precise way to understand the features of instabilities in two-component systems such as nuclear matter is to consider the equilibrium phase transition together with the nuclear collisions driving such phase transition at intermediate energies. In this work we are interested in the quantal effects on the growth of instabilities in infinite nuclear matter around the equilibrium. The relation to thermodynamic properties of infinite nuclear matter is obtained by discarding the Coulomb interactions. Thus the equilibrium phase transition and the characteristics of the collective modes will be discussed including the quantum effects.

In the previous years, several theoretical models have been used in order to study the nuclear dynamics at intermediate energies. Especially the much employed Boltzmann-Uehling-Uhlenbeck (BUU) model provides a good basis for describing dynamics of small density fluctuations around the equilibrium [4]. The BUU equation includes the mean-field and the hard collisions. Under certain kinematic conditions, a nuclear collision can produce physical situations in which bulk or surface instabilities take place [5, 6]. In Ref. [5], the central heavy-ion collisions at intermediate energy are simulated using the nuclear BUU transport theory and it is shown that the nuclear bubbles and the disks formed during the collision break up into several fragments due to the surface instabilities. A sheet of liquid, stable in

the limit of non-interacting surfaces, becomes unstable due to surface-surface interactions. In Ref. [6], the intermediate energy heavy ion collisions are studied again by the means of BUU equation and it is seen that the intermediate-mass fragments occur through the entire nuclear volume.

Semi-classical kinetic equations for the one–body phase–space density provide a powerful tool for studying the dynamics of complex processes occurring in nuclear collisions [4]. However, these equations in their original version give a deterministic description for the evolution of the one–body phase–space density and their solution represents the mean value of this density at each time. These semi-classical transport theories account for the residual interactions in only an average manner and they are only well suited for small density fluctuations. Therefore such a description is inadequate for the processes such as nuclear collisions in which the fluctuations about the phase-space density are believed to play an important role. In the last decade, an extension of the transport theory has been proposed [7, 8]. In Ref. [7], the BUU approach is extended in order to incorporate the fluctuations. The evolution of the single-particle density is considered as a "generalized Langevin process" in which the correlated part of the collision term acts as a "random force" generating the fluctuations. The correlation function of the random force is calculated in the semi-classical approximation. The result is a "stochastic transport equation" for the fluctuating single-particle density. In Ref [8], even though the starting point is identical with that of Ref. [7], the methods are different. In both studies, the fluctuations induced by the two-body collisions is treated as a Langevin process. The correlation function associated with

the one-particle distribution may then be deduced from the properties of the fluctuating force. This approach, that incorporates a fluctuating stochastic term into the kinetic equation, is usually known as the Boltzmann–Langevin equation, and it was originally applied to the treatment of hydrodynamic fluctuations in the theory of classical fluids [9]. While an explicit expression for the correlation of the fluctuating force is derived and this is defined as the source term for the fluctuations in Ref. [7], this term appears as the diffusion coefficient in the equations of Ref. [8]. In addition to this term, a degradation term is derived, using the stochastic properties of the basic two-body collision term. This restoring term acts to saturate the growth of the fluctuations and is responsible for establishing equilibrium.

The nuclear Boltzmann-Langevin model gives a semi-classical description of the nuclear system in terms of its reduced one particle phase-space density whose evolution in time is governed by the combined action of the effective one-body field $h[\rho]$ and the residual two-body collisions between individual nucleons, $I_0[\rho]$ [10].

Among microscopic approaches, the Boltzmann-Langevin (BL) equation is one of the most suitable to describe the large density fluctuations in a nuclear system. This approach incorporates a stochastic term into the kinetic equation and includes fluctuations in the evolution of density [7, 8].

Many studies have been carried out by the means of the semi-classical BL model to understand the early development of the spinodal instabilities in nuclear matter [11-13]. A simple transport equation determines the dynamics of the collective modes associated with density fluctuations. This equation includes the source term arising from the stochastic part of the collision integral. This term causes the collective modes of the system. Also the mean field that gives rise to propagation of the modes is included in the transport equation. Ref. [11] shows that the application of linear response treatment to the Boltzmann-Langevin theory provides a relatively simple and complete understanding of the early development of the one-body phase-space density in nuclear matter, including its correlation function. Within such an approach it is possible to describe the time evolution of the correlated fluctuations created by the stochastic two-body collisions in the system. It is seen that two-time correlation function contains no information on the spontaneous creation of the fluctuations but for stable matter it exhibits the effects of both Landau damping, due to the effective field, and the collisional damping. Also it reflects the characteristic times for the amplification of existing fluctuations for the unstable systems. The evolution of equal-time correlation function is used to determine the source term governing the growth rate of the unstable modes in the system. This has been illustrated in the case of spinodal instabilities in idealized two-dimensional matter [11].

In this study we will investigate the collective modes in infinite nuclear matter by solving the BL equation. Since it is known that the fastest growing and the predominant collective modes have wave numbers comparable to the Fermi

momentum [11], the quantal effects are said to have an important influence on the growth of spinodal instabilities in nuclear matter. So, we will be interested in the quantal determination of the dynamics of the density fluctuations. Therefore, we will neglect the stochastic part of the BL equation which arises from the collision effects.

We will start with the quantal BL equation for the single density matrix $\hat{\rho}$ and use the linearization to investigate the small density fluctuations of the single particle density matrix around a finite temperature. Mean-field evolution will be determined in terms of an effective one-body Hamiltonian $h[\rho]$ which includes a density dependent mean-field potential $U[\rho]$.

Then, in a quantal description we will obtain a dispersion relation for the frequency of the collective mode corresponding to the wave number $\boldsymbol{k}$. For three types of Skyrme potentials, the dispersion relation will be evaluated. And the results of the quantal description and the semi-classical approach will be compared for three types of Skyrme potentials.

After the investigation of the effects of quantal description on the collective modes, we will look at the spinodal boundary for three mean-field potentials and we observe the quantal effects on the phase diagrams.

CHAPTER 2

FORMALISM

In infinite nuclear matter, the collective modes are characterized by a wave number $\boldsymbol{k}$. The characteristic frequency of the collective mode corresponding to a given wave number is determined by a semi-classical dispersion relation. It is known that the fastest developing modes are approximately characterized by wave numbers comparable to the Fermi momentum [11]. Therefore, the quantal effects associated with the mean field evolution can have important influence on the growth of instabilities.

The quantal BL equation for the single particle density matrix provides a suitable framework for studying the dynamics of density fluctuations in nuclear systems which is given as [14]

$$i\hbar\frac{\partial\hat{\rho}(t)}{\partial t}-\left[\hat{h}[\hat{\rho}],\hat{\rho}(t)\right]=\hat{K}[\hat{\rho}]+\delta\hat{K}(t) \tag{2.1}$$

where $\hat{h}[\hat{\rho}]$ is an effective one-body Hamiltonian operator

$$\hat{h}[\hat{\rho}]=-\frac{\hbar^2}{2m}\hat{\nabla}^2+\hat{U}[\hat{\rho}] \tag{2.2}$$

and $\hat{U}[\hat{\rho}]$ is density dependent mean-field potential. The additional field will induce density fluctuations with respect to the mean density. At time t=0, the system has a density fluctuation $\delta\rho(t=0)$, with $\delta\rho(t)=\rho(t)-\rho_0$ where ρ_0 is the density of the reference homogeneous state towards which the system relaxes. With the substitution

$$\hat{\rho} \to \hat{\rho}_0 + \delta\hat{\rho}$$

we obtain

$$\hat{U}[\hat{\rho}] \to \hat{U}[\hat{\rho}_0] + \delta\hat{U}$$

and

$$\hat{h}[\hat{\rho}] \to -\frac{\hbar^2}{2m}\hat{\nabla}^2 + \hat{U}[\hat{\rho}+\delta\hat{\rho}] = -\frac{\hbar^2}{2m}\hat{\nabla}^2 + \hat{U}(\hat{\rho}_0) + \delta\hat{U} = \hat{h}_0 + \delta\hat{U} \quad . \qquad (2.3)$$

Within a linear approximation for the stochastic mean-field, the small density fluctuations $\delta\hat{\rho}$ of the single particle density matrix around a finite temperature equilibrium density matrix $\hat{\rho}_0$ are determined by the quantal BL equation

$$i\hbar\frac{\partial}{\partial t}[\hat{\rho}_0+\delta\hat{\rho}] - [\hat{h}_0+\delta\hat{U}, \hat{\rho}_0+\delta\hat{\rho}] = K[\hat{\rho}_0+\delta\hat{\rho}] + \delta\hat{K}(t) \quad . \qquad (2.4)$$

By employing Eq. 2.4 for ρ_0, i.e. at equilibrium and ignoring the multiplied fluctuations, we obtain

$$i\hbar\frac{\partial\delta\hat{\rho}}{\partial t} - [\hat{h}_0, \delta\hat{\rho}] - [\delta\hat{U}, \hat{\rho}_0] = I_0\delta\hat{\rho} + \delta\hat{K}_0 \qquad (2.5)$$

where $\hat{h}_0$ is the mean field Hamiltonian and $\hat{\rho}_0$ is the single particle density matrix both at equilibrium state, $\delta\hat{U}$ is the fluctuating part of Hamiltonian, $I_0\delta\hat{\rho}$ is the linearized approximation to the two-body collision term, and $\delta\hat{K}_0$ describes the rate of fluctuations generated in the equilibrium state. This model provides a quantal basis to study the early evolution of the spinodal instabilities in nuclear matter. In this work, we are mainly interested in studying the quantal effect on the growth of instabilities in infinite nuclear matter, therefore we neglect the right-hand-side of Eq. 2.5, and obtain

$$i\hbar\frac{\partial\delta\hat{\rho}(t)}{\partial t}-\left[\hat{h}_0,\delta\hat{\rho}\right]=\left[\delta\hat{U},\hat{\rho}_0\right]. \tag{2.6}$$

Since we assume that the equilibrium state is uniform, the equilibrium single particle density matrix is diagonal in the plane wave representation, $\left\langle \boldsymbol{p}_1\left|\hat{\rho}_0\right|\boldsymbol{p}_2\right\rangle=\delta(\boldsymbol{p}_1-\boldsymbol{p}_2)\rho_0(\boldsymbol{p}_1)$. After writing all the terms in Eq. 2.6 in plane wave representation in momentum space and performing a Fourier transform with respect to time, the details of which is presented in Appendix A, Eq. 2.6 becomes

$$(\hbar\omega-\varepsilon_{p_1}+\varepsilon_{p_2})\delta\rho(\boldsymbol{p}_1,\boldsymbol{p}_2;\omega)=\left[\rho_0(\boldsymbol{p}_2)-\rho_0(\boldsymbol{p}_1)\right]\delta U(\boldsymbol{p}_1,\boldsymbol{p}_2;\omega)\ , \tag{2.7}$$

where $\delta\rho(\boldsymbol{p}_1,\boldsymbol{p}_2;\omega)$ and $\delta U(\boldsymbol{p}_1,\boldsymbol{p}_2;\omega)$ denote the Fourier transform of the fluctuating part of the single particle density matrix and of the mean-field matrix, respectively,

$$\delta\rho(\boldsymbol{p}_1,\boldsymbol{p}_2;\omega)=\int e^{i\omega t}<\boldsymbol{p}_1\mid\delta\hat{\rho}(t)\mid\boldsymbol{p}_2>dt\ , \tag{2.8.a}$$

$$\delta U(\boldsymbol{p}_1, \boldsymbol{p}_2; \omega) = \int e^{i\omega t} < \boldsymbol{p}_1 \mid \delta\hat{U}(t) \mid \boldsymbol{p}_2 > dt \ . \qquad (2.8.b)$$

In order to evaluate the matrix element of the mean-field, we write the momenta in Eq. 2.7 as $\boldsymbol{p}_1 = \boldsymbol{p} + \hbar\boldsymbol{k}/2$ and $\boldsymbol{p}_2 = \boldsymbol{p} - \hbar\boldsymbol{k}/2$. When the effective mean-field is generated from the local density $n(\boldsymbol{r})$ with a finite range interaction $g(|\boldsymbol{r}|)$, then the potential is given as $U(n) = g \otimes \tilde{U} = \int d^3r' g(|\boldsymbol{r} - \boldsymbol{r}'|)\tilde{U}[n(\boldsymbol{r}')]$ where $\tilde{U}[n(\boldsymbol{r})]$ is a function of local density and $g(|\boldsymbol{r}|) = (\mu^2 e^{-\mu r})/4\pi r$ is used as convolution function with $\mu = 0.8\,\mathrm{fm}^{-1}$. Then, the fluctuating part of the mean-field can be expressed as

$$\delta U(\boldsymbol{p} + \frac{\hbar\boldsymbol{k}}{2}, \boldsymbol{p} - \frac{\hbar\boldsymbol{k}}{2}; \omega) = \frac{\partial U(\boldsymbol{k})}{\partial n} \delta n(\boldsymbol{k}, \omega) \qquad (2.9)$$

where $U(k) = g(k)\tilde{U}[n_0]$ and $g(k) = (2\pi)^{-3}\mu^2/(k^2 + \mu^2)$ is the Fourier transform of the convolution function $g(r)$. The details of the derivation is given in Appendix B.2. In the above equation $\delta n(\boldsymbol{k}, \omega)$ denotes the Fourier transform of the local density fluctuations in space and time as

$$\delta n(\boldsymbol{k}, \omega) = \int d\boldsymbol{r} dt e^{-i\boldsymbol{k}\cdot\boldsymbol{r}} e^{i\omega t} \delta n(\boldsymbol{r}, t) = \int \frac{d\boldsymbol{p}}{(2\pi\hbar)^3} \delta\rho(\boldsymbol{p} + \frac{\hbar\boldsymbol{k}}{2}, \boldsymbol{p} - \frac{\hbar\boldsymbol{k}}{2}; \omega) \ , \quad (2.10)$$

where the right-hand-side of this equation is obtained by calculating the matrix element of the fluctuating part of the density matrix between the single particle states with $\boldsymbol{p}_1 = \boldsymbol{p} + \hbar\boldsymbol{k}/2$, $\boldsymbol{p}_2 = \boldsymbol{p} - \hbar\boldsymbol{k}/2$ in Eq. 2.8.a, and integrating over $\boldsymbol{p}$

after performing the Fourier transform with respect to time which is shown in detail in Appendix B.1.

After writing Eq. 2.7 with $\boldsymbol{p}_1 = \boldsymbol{p} + \hbar\boldsymbol{k}/2$, $\boldsymbol{p}_2 = \boldsymbol{p} - \hbar\boldsymbol{k}/2$, performing integration with respect to $\boldsymbol{p}$ and using Eq. 2.9 and Eq. 2.10 for the expressions in the momentum integral, we then obtain a quantal dispersion relation for the frequency of the collective mode corresponding to the wave number $\boldsymbol{k}$ as

$$1 = \frac{\partial U(\boldsymbol{k})}{\partial n} \int \frac{d\boldsymbol{p}}{(2\pi\hbar)^3} \frac{\rho_0(\boldsymbol{p} - \hbar\boldsymbol{k}/2) - \rho_0(\boldsymbol{p} + \hbar\boldsymbol{k}/2)}{(\hbar\omega_k - \varepsilon_{\boldsymbol{p}+\hbar\boldsymbol{k}/2} + \varepsilon_{\boldsymbol{p}-\hbar\boldsymbol{k}/2})} \ . \qquad (2.11)$$

This quantal dispersion relation can be evaluated exactly at zero temperature. However, for finite temperature it must be studied numerically. The results are discussed in Chapter 3.

CHAPTER 3

RESULTS AND DISCUSSION

In this chapter we analyze the dispersion relation obtained in the previous chapter by considering three different finite range interactions. The characteristic frequencies of the collective modes are solved implicitly by using a numerical method. Finite temperature T= 3 MeV and a constant density value $n_0 = 0.05$ fm^{-3} will be used to determine the characteristic frequencies for the unstable nuclear matter. Then, the boundary of the spinodal region is determined in the (ρ, T) plane again using the three different effective interactions. For the phase diagrams the frequency is chosen to satisfy the spinodal boundary condition which is $\omega_k = 0$. Both in the dispersion relation and in the phase diagram, the quantal and the semi-classical results are compared and it is demonstrated that the inclusion of the quantal effects in the mean-field propagation changes significantly the nuclear dispersion relation and the boundary of the spinodal region.

In infinite nuclear matter, the collective modes are characterized by a wave number $\boldsymbol{k}$ and the corresponding frequencies occur in pairs as $\pm\omega_k$. The characteristic frequencies are real for the stable modes and imaginary for the

unstable modes, in which case they are written as $\omega_k = i/\tau_k$ where $\pm\tau_k$ is the characteristic growth or decay time of the mode. For the unstable modes, the plane wave representation of the system is denoted in terms of $e^{\mp(1/\tau_k)t}$ instead of $e^{\pm i\omega_k t}$.

3.1. Zero Temperature

Before investigating the finite temperature condition we will first look at the zero temperature case. In the zero temperature limit, the Fermi distribution reduces to a step function [15] shown in Fig. 3.1.

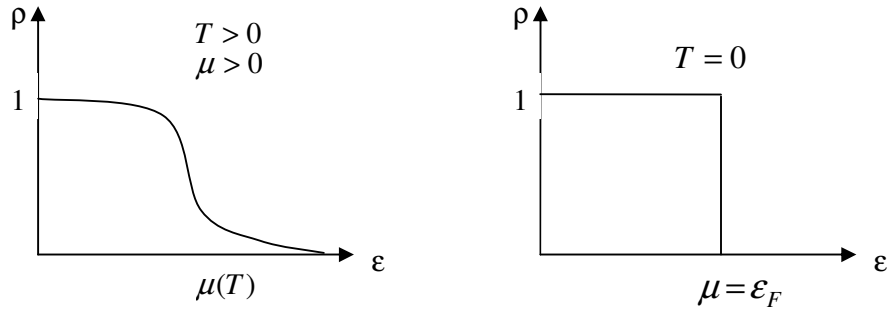

$$\rho_0 = \frac{1}{e^{(\varepsilon-\mu)/k_B T}+1} \qquad \rho_0 = \theta(\varepsilon_F - \varepsilon)$$

Figure 3.1: Schematic distribution functions $\rho(\varepsilon)$ for an ideal Fermi gas at various temperatures.

This limit can be expressed as

$$\rho_0 = \frac{1}{e^{(\varepsilon-\mu)/k_B T}+1} \underset{T\to 0}{\rightarrow} \begin{Bmatrix} 0 & for & \varepsilon > \mu \\ & & \\ 1 & for & \varepsilon < \mu \end{Bmatrix} = \theta(\mu - \varepsilon) \ . \qquad (3.1)$$

At zero temperature the chemical potential is equal to the Fermi energy $\mu = \varepsilon_F$. Therefore, the density term in the dispersion relation becomes $\rho_0 = \theta(\varepsilon_F - \varepsilon)$, where $\varepsilon_p = p^2 / 2m$, thus for zero temperature we have the relations

$$\rho_0(\boldsymbol{p}) = \theta(\frac{{p_F}^2}{2m} - \frac{p^2}{2m}) \ , \tag{3.2}$$

$$\rho_0(\boldsymbol{p} - \hbar\boldsymbol{k}/2) = \theta(\frac{{p_F}^2}{2m} - \frac{(\boldsymbol{p} - \hbar\boldsymbol{k}/2)^2}{2m}) = \theta(p_F - |\boldsymbol{p} - \hbar\boldsymbol{k}/2|) \ , \tag{3.3}$$

$$\rho_0(\boldsymbol{p} + \hbar\boldsymbol{k}/2) = \theta(\frac{{p_F}^2}{2m} - \frac{(\boldsymbol{p} + \hbar\boldsymbol{k}/2)^2}{2m}) = \theta(p_F - |\boldsymbol{p} + \hbar\boldsymbol{k}/2|) \ . \tag{3.4}$$

Then, with these expressions in the integrand, Eq. 2.11 becomes

$$1 = \frac{\partial U(\boldsymbol{k})}{\partial n} \int \frac{d\boldsymbol{p}}{(2\pi\hbar)^3} \left(\frac{\theta(p_F - |\boldsymbol{p} - \hbar\boldsymbol{k}/2|)}{\hbar\omega_k - \hbar\boldsymbol{k}.\boldsymbol{p}/m} - \frac{\theta(p_F - |\boldsymbol{p} + \hbar\boldsymbol{k}/2|)}{\hbar\omega_k - \hbar\boldsymbol{k}.\boldsymbol{p}/m} \right) \ , \tag{3.5}$$

which is discussed in detail in Appendix C.1. This integral is also evaluated in Appendix C.1 and the quantal dispersion relation in Eq. 2.11 can be written for $T = 0$ as

$$1 = \frac{\partial U(k)}{\partial n} \frac{2\pi 2 p_F m}{(2\pi\hbar)^3} \left\{ -\frac{1}{2} + \frac{1}{8s_0} \left[(s + s_0)^2 - 1 \right] \ln \frac{s + s_0 + 1}{s + s_0 - 1} \right.$$
$$\left. - \frac{1}{8s_0} \left[(s - s_0)^2 - 1 \right] \ln \frac{s - s_0 + 1}{s - s_0 - 1} \right\} \ , \tag{3.6}$$

where $s = m\omega_k / kp_F$ and $s_0 = \hbar k / 2p_F$ are dimensionless variables. This expression can further be rearranged as

$$\frac{1}{F_0(k)}+\frac{1}{2} = \left\{ \frac{1}{8s_0}\left[(s+s_0)^2-1\right] \ln\frac{s+s_0+1}{s+s_0-1} \right.$$

$$\left. -\frac{1}{8s_0}\left[(s-s_0)^2-1\right] \ln\frac{s-s_0+1}{s-s_0-1} \right\} \qquad (3.7)$$

where $F_0(k)=\left[\partial U(k)/\partial n\right]\ (3n_0/2\varepsilon_F)$, $n_0 = 2{k_F}^3/3\pi^2$ and $\varepsilon_F = {p_F}^2/2m$.

In the limit of $\hbar$ is going to zero, Eq. 3.7 reduces to the semi-classical dispersion relation at zero temperature in the form

$$\frac{1}{F_0(k)}+1=\frac{s}{2}\ln\frac{s+1}{s-1} \ , \qquad (3.8)$$

the derivation of which is presented in Appendix C.1.1.

3.2. Finite Temperature

At finite temperature the density term in the dispersion relation becomes

$$\rho_0 = \frac{1}{e^{(\varepsilon-\mu)/k_BT}+1} \qquad (3.9)$$

which is a finite temperature Fermi-Dirac distribution function and the chemical potential is determined as $\mu=\varepsilon_F\left[1-(\pi^2/12)(k_BT/\varepsilon_F)^2\ \right]$ in terms of Fermi energy [15]. The Fermi energy is calculated in terms of local density in Appendix D. We take the equilibrium local density as $n_0 = 0.05$ fm^{-3} and $T = 3\,\text{MeV}$ in the dispersion relation to obtain the frequency growth rate graphs.

We determine the characteristic frequencies of the collective modes by solving the quantal dispersion relation Eq. 2.11 at finite temperatures. The angular part of the integral in the dispersion relation is evaluated in Appendix C.2. We take the frequency as $\omega_k = i/\tau_k$ for unstable modes and analytic calculation gives

$$1 = \frac{\partial U(k)}{\partial n} 2\pi \int \frac{dp}{(2\pi\hbar)^3} \rho_0(p) p \frac{2m}{2\hbar k} \left\{ \ln\left|(\hbar/\tau_k)^2 + (-2\hbar pk/2m + \hbar^2 k^2/2m)^2\right| - \ln\left|(\hbar/\tau_k)^2 + (2\hbar pk/2m + \hbar^2 k^2/2m)^2\right| \right\}. \quad (3.10)$$

The remaining part of the integral is calculated numerically. For the quantal calculations the density is taken as in Eq. 3.9. For the semi-classical limit it is used as $\rho_0 = e^{(\mu-\varepsilon)/k_B T}$, which is the semi-classical or high-temperature limit of the Fermi distribution and known as Boltzmann distribution [15].

In the calculations we employ three types of Skyrme interactions [16]:

i) Full Skyrme potential for symmetric nuclear matter

$$U(\rho) = t_0(1 + \frac{1}{2}x_0)\rho - t_0(\frac{1}{2} + x_0)\frac{\rho}{2} + \frac{1}{12}t_3\rho^\alpha\left[(2+\alpha)(1+\frac{1}{2}x_3)\rho - 2(\frac{1}{2}+x_3)\frac{\rho}{2} - \alpha(\frac{1}{2}+x_3)\frac{\rho}{2} \right], \quad (3.11)$$

where $t_0 = -2488.91\,\text{MeV.fm}^3$, $t_3 = 13777\,\text{MeV.fm}^{7/2}$, $x_0 = 0.834$ $x_3 = 1.354$ and $\alpha = 1/6$.

ii) Simplified Skyrme potential for symmetric nuclear matter

$$U(\rho) = (-124MeV)\frac{\rho}{\rho_0} + (70.5MeV)(\frac{\rho}{\rho_0})^2, \quad (3.12)$$

which is a repulsive potential of high compressibility κ = 380 MeV.

iii) Simplified Skyrme potential for symmetric nuclear matter

$$U(\rho) = (-356MeV)\frac{\rho}{\rho_0} + (303MeV)(\frac{\rho}{\rho_0})^{7/6} , \qquad (3.13)$$

which is a less repulsive potential with κ = 200 MeV.

In the above equations ρ_0 denotes the normal nuclear matter density which is ρ_0=0.16 fm^{-3}.

The results are discussed in Section 3.3 and Section 3.4.

3.3 Dispersion Relations

We studied the dispersion relation at finite temperature by means of numerical integration techniques, and we obtained the growth rate of the unstable modes for three different Skyrme forces.

Fig. 3.2 shows the growth rate of the unstable modes as a function of the wave number in the spinodal region, corresponding to $n_0 = 0.05$ fm^{-3} and $T = 3$MeV, calculated with the effective interaction in Eq. 3.11. The solid line shows the quantal result with the finite range interaction. The dashed line shows the semi-classical result with the same finite range interaction. The dotted line is the quantal result obtained with a local mean field which does not include the convolution term. The distribution of the collective modes is between k=0-2 fm^{-1} concentrated around 1 fm^{-1} in the quantal result. It corresponds to $\lambda \approx 6$ fm, which

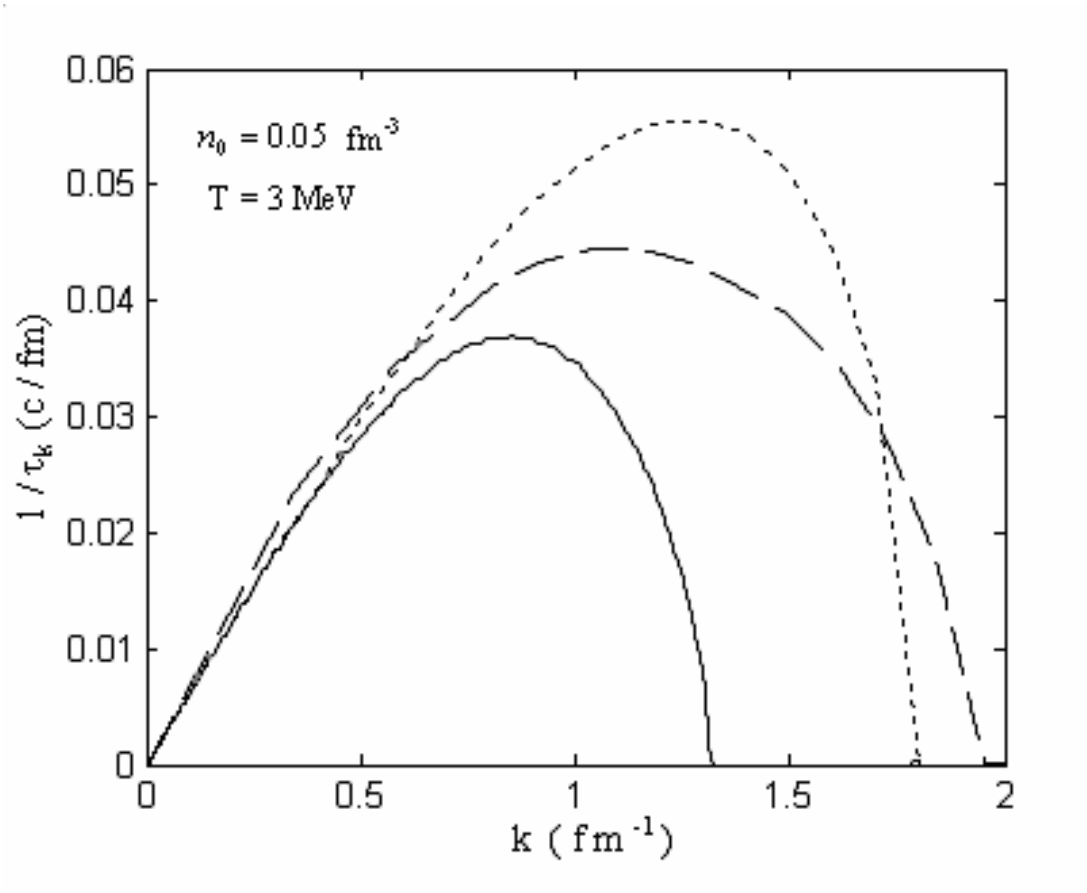

Figure 3.2: The dispersion relation for the unstable nuclear matter at $n_0 = 0.05\,\mathrm{fm}^{-3}$ and $T = 3\,\mathrm{MeV}$, with the full Skyrme force.

is the wavelength of fastest growing collective modes as seen from the graph. These are the most important collective modes which characterizes the growth of the expanding nuclear system. While the growth rate of the fastest modes are around 0.035 c/fm in the quantal case, it is around 0.046 c/fm in the semi-classical result. The maximum of the dispersion relation is reduced by a factor of about 2/3, the modes grow slowly with the quantum effects.

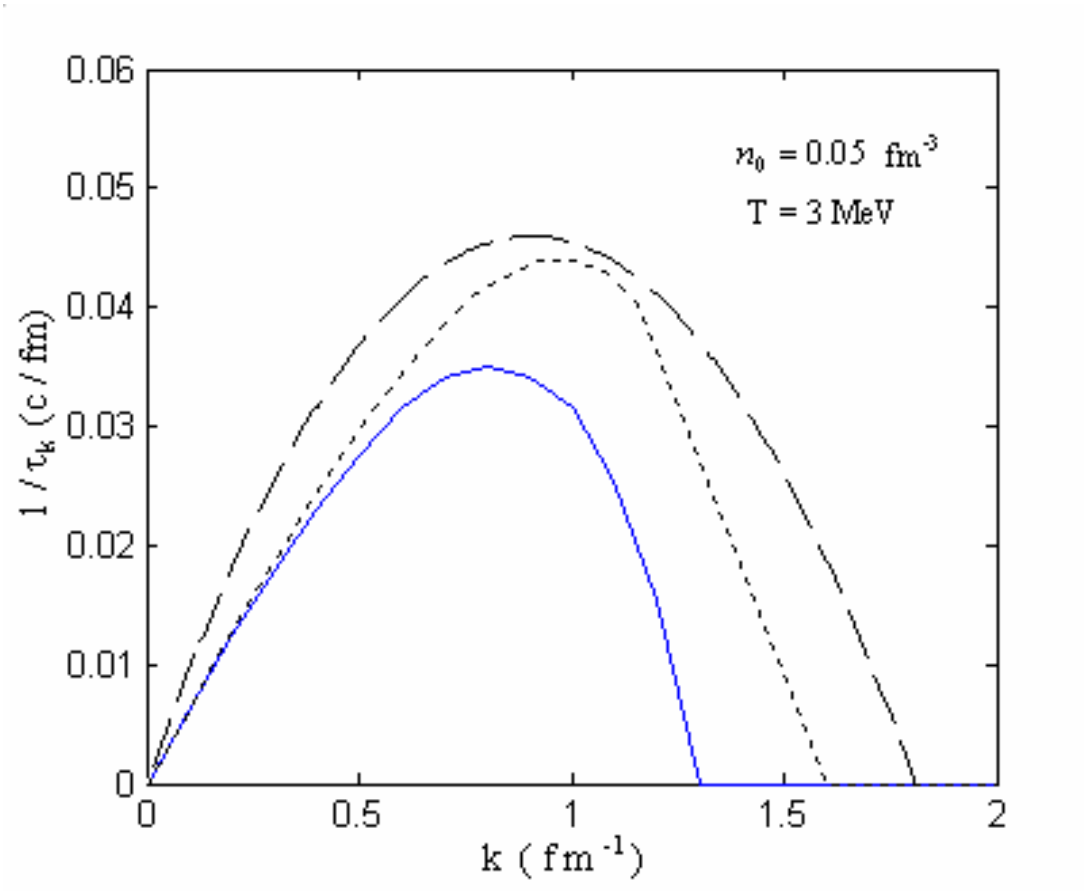

Figure 3.3: The dispersion relation for the unstable nuclear matter at $n_0 = 0.05\,\mathrm{fm}^{-3}$ and $T = 3\,\mathrm{MeV}$, with the second type Skyrme force.

Fig. 3.3 and Fig. 3.4 shows the same quantities calculated with the other two effective interactions given by Eq. 3.12 and Eq. 3.13, respectively. As it is seen from the figures, the dispersion relation does not depend very strongly on the employed effective interaction, but it is substantially modified by the quantal effect. The unstable modes are confined to a narrower range centered around a wavelength $\lambda \approx 8-10\,\mathrm{fm}$, as compared to a broader range concentrated around $\lambda \approx 6$ fm, in the semi-classical case. The most unstable collective modes, which

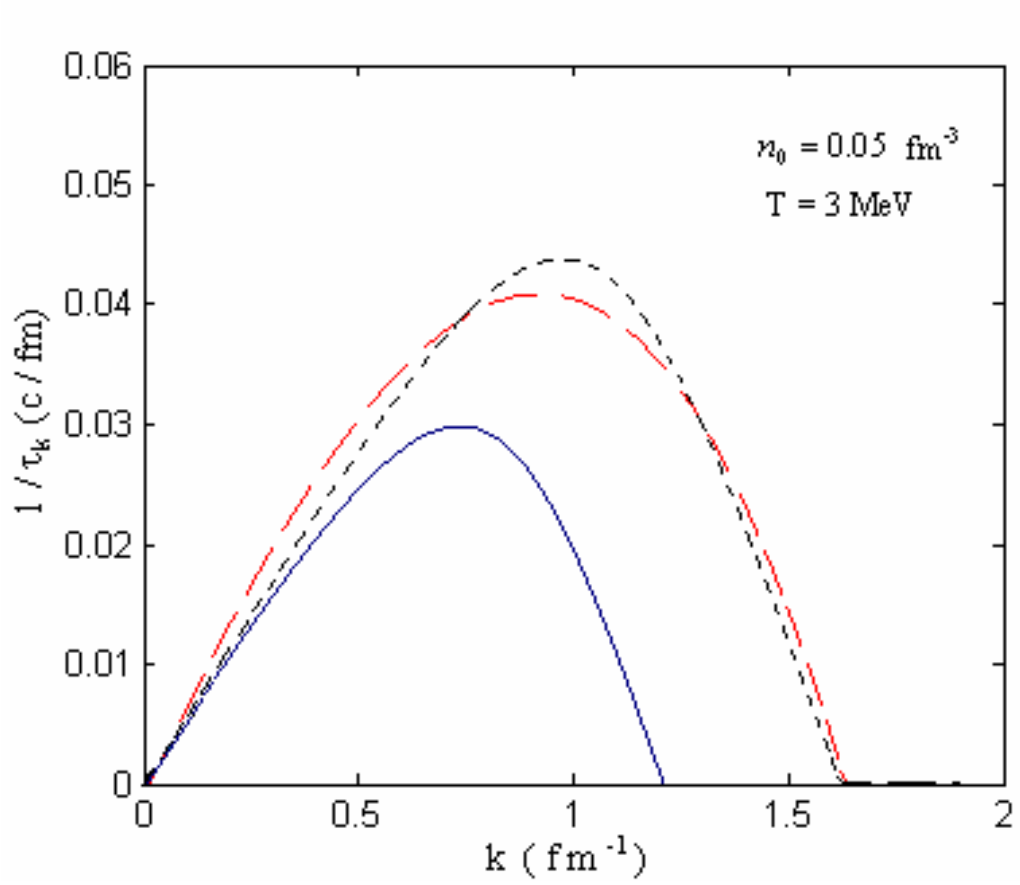

Figure 3.4: The dispersion relation for the unstable nuclear matter at $n_0 = 0.05\,\mathrm{fm}^{-3}$ and $T = 3\,\mathrm{MeV}$, with the third type Skyrme force.

essentially determine the predominant size of the primary clusters, are shifted to longer wavelengths than those obtained in a semi-classical description with the same effective interaction. Since the larger wavelength means bigger sizes and fewer amounts of particles for a system, it is concluded that the system has tendency to break into larger sizes of clusters when the quantal effects are included.

Also the maximum of the dispersion relation is reduced by the quantum effects about a factor of 2/3. Therefore fluctuations take more time to develop when

the quantum effects are introduced. So, the most unstable modes show up later in larger wavelengths with the inclusion of the quantum effects.

3.4 Phase Diagrams

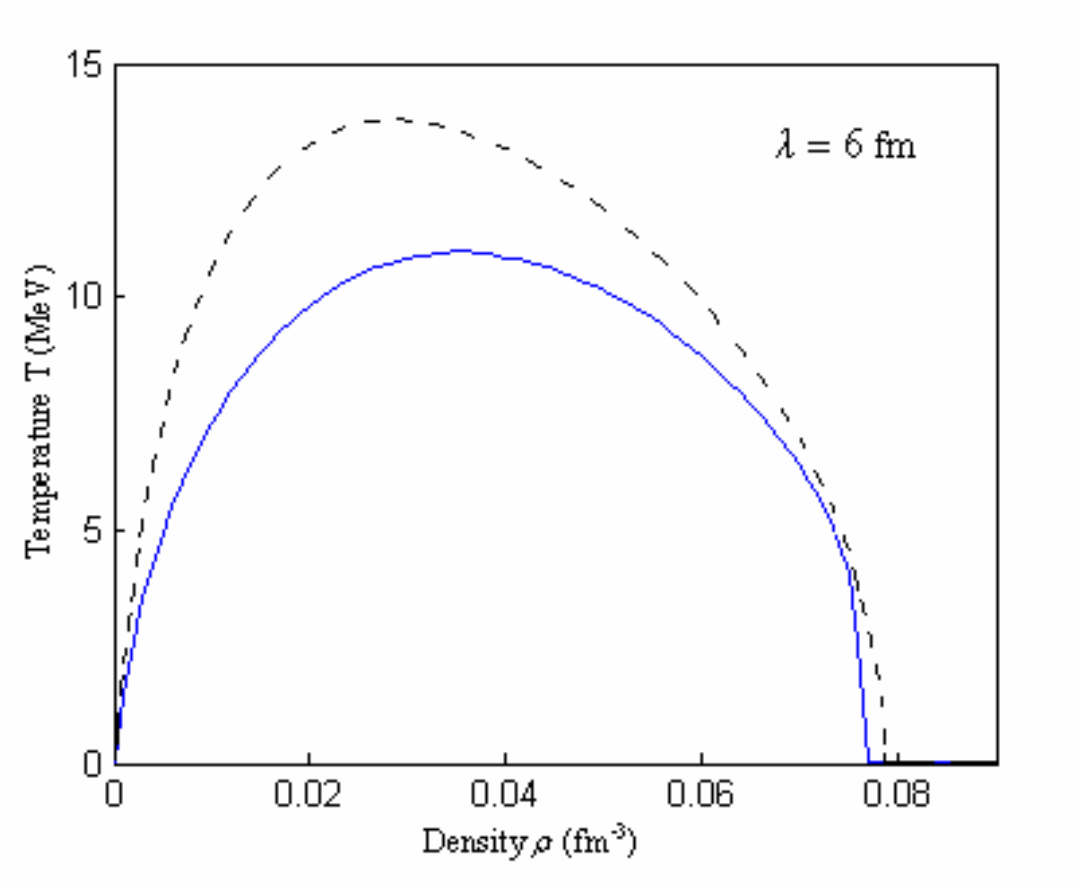

Figure 3.5: Phase diagram. The boundaries of the spinodal region in the (ρ, T) plane associated with the wavelength $\lambda = 6$ fm, obtained in the quantal (solid line) and in the semi-classical (dashed line) case, with the full Skyrme force.

Fig. 3.5, Fig. 3.6 and Fig. 3.7 show the boundary of spinodal region in the (ρ, T) plain corresponding to a mode with a wavelength $\lambda \approx 6$ fm. The solid and the dashed lines are the quantal and the semi classical results, respectively,

obtained with the three effective interactions introduced above. It is seen that the spinodal region shrinks to a smaller size in the quantal case, indicating that the mode is quite suppressed by quantal effects. Therefore, finite size effects should be more important when quantum effects are introduced.

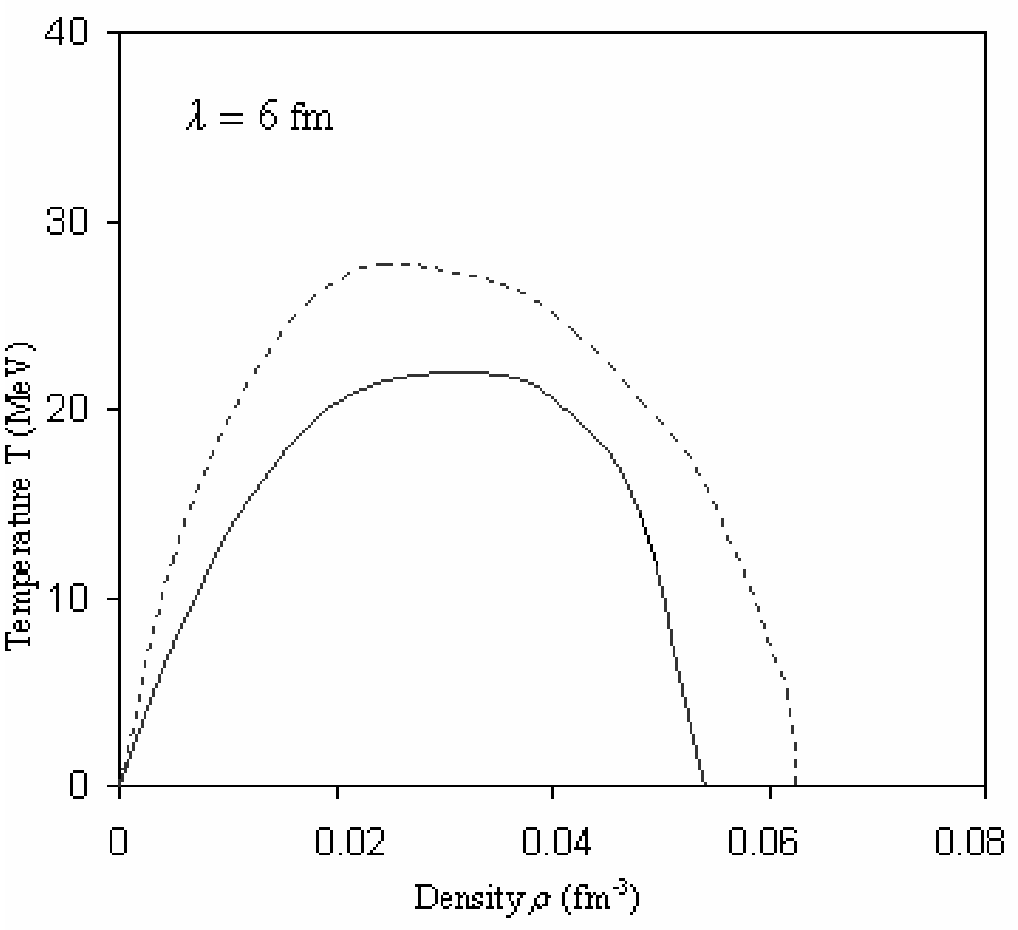

Figure 3.6: Phase diagram. The boundaries of the spinodal region in the (ρ, T) plane associated with the wavelength $\lambda = 6$ fm, obtained in the quantal (solid line) and in the semi-classical (dashed line) case, the second type Skyrme force.

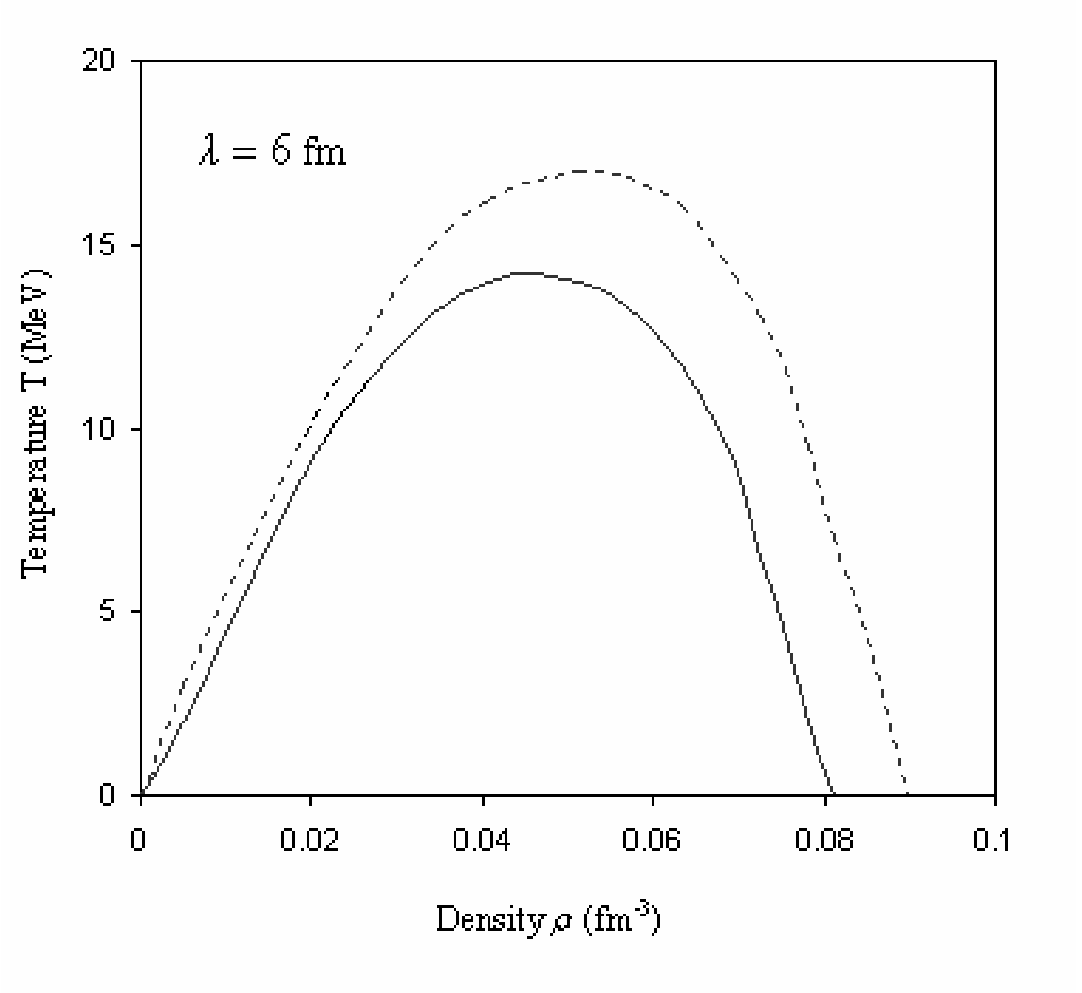

Figure 3.7: Phase diagram. The boundaries of the spinodal region in the (ρ, T) plane associated with the wavelength $\lambda = 6$ fm, obtained in the quantal (solid line) and in the semi-classical (dashed line) case, the third type Skyrme force.

CHAPTER 4

CONCLUSIONS

In this study, the instability of a hot infinite nuclear matter is considered. Quantal effects are observed within a linearized Boltzmann-Langevin transport model. The growth rates of the unstable modes in nuclear matter are investigated using a quantal dispersion relation. These results exhibit the characteristics of the collective modes and the range of spinodal region for infinite nuclear matter. It is seen that for a density around the 30% of normal nuclear matter density and for temperature around 3 MeV the relevant most important modes become unstable with similar growth rates around 0.04-0.06 c/fm, but these growth rates are reduced to the values around 0.03 c/fm by the quantal effects. The spinodal boundaries are also similar under different finite range interactions, but again reduced by inclusion of the quantum effects.

If we compare our results with some studies carried out for finite nuclear matter including the surface effects [17, 18], we see that the bulk modes have a smaller spinodal region than the surface modes. That is, finite nuclear matter have larger spinodal region, reaching out to densities and temperatures way beyond the spinodal line for bulk instabilities. In [18], early development of the instabilities in

a dilute nuclear source is investigated using a finite temperature quantal approach for different systems. The growth rates of the unstable collective modes are determined by solving a dispersion relation, which is obtained by parametrizing the transition density in terms of its multipole moments. As a result, only a finite number of multipole moments becomes unstable, and the number of the unstable collective modes increases with the size of the source. Calculations indicate that for an expanding source, unstable modes show a transition from surface to volume character.

Although multifragmentation has been observed for many years, its experimental knowledge was strongly improved only recently with the advent of powerful devices built in the last decade. The properties of highly excited nuclear sources which undergo a simultaneous disassembly into particles are found to sign the presence of a gas phase. For heavy nuclear sources produced in the Fermi energy domain, which undergo a simultaneous disassembly into particles and fragments, fragment size correlations bring out the origin of multifragmentation as the spinodal instabilities which develop in the unstable coexistence region of the phase diagram of nuclear matter [3].

The results of this study, together with the similar calculations carried out for finite nuclear matter [18], show that the inclusion of the quantal effect in the mean-field propagation changes significantly the nuclear dispersion relation and the boundary of the *k*-dependent spinodal region. The characteristic growth rates of the unstable modes, in particular with wave numbers larger than the Fermi momentum,

are strongly suppressed and the size of the spinodal zone corresponding to these modes is reduced by the quantal effect. As a result, the most unstable collective modes are shifted to longer wave lengths than in a semi-classical description with the same effective interaction. Therefore, the quantal effect in the mean-field evolution appears to be important for a quantitative description of the spinodal instabilities of an expanding nuclear system.

REFERENCES

[1] V. A. Karnaukhov, et al., nucl-ex/0310009 (2003).

[2] V. Baran et al., Invited talk at the Conference: "Structure of the Nucleus at the Dawn of the Century", Bologna, Italy, May 29-June 3, nucl-th/0009080 (2000).

[3] B. Borderie, Invited talk at the Conference: "Structure of the Nucleus at the Dawn of the Century", Bologna, Italy, May 29-June 3, nucl-ex/0102016 (2000).

[4] G.F. Bertsch and S. Das Gupta, Phys. Rep. **160**, 190 (1988).

[5] L.G. Moretto, K. Tsuo, M. Colonna and G.J. Wozniak Phys. Rev. Lett. **69**, 1884 (1992).

[6] W. Bauer, G.F. Bertsch and H. Shultz, Phys. Rev. Lett. **69**, 1888 (1992).

[7] S. Ayik and C. Gregoire, Phys. Lett. **B 212**, 269 (1988); Nucl. Phys. **A 513**, 187 (1990).

[8] J. Randrup and B. Remaud, Nucl. Phys. **A 514**, 339 (1990).

[9] M. Bixon and R. Zwanzig, Phys. Rev. **187**, 267 (1969).

[10] J. Randrup, Nucl. Phys. **A 583**, 329-332 (1995).

[11] M. Colonna, Ph. Chomaz and J. Randrup, Nucl. Phys. **A 567**, 637 (1994).

[12] D. Kiderlen and H. Hofmann, Phys. Lett. **B 332**, 8 (1994).

[13] S. Ayik and J. Randrup Phys. Rev. **C 50**, 2947 (1994).

[14] S. Ayik, M. Colonna and Ph. Chomaz, Phys. Lett. **B 353**, 417 (1995).

[15] A. L. Fetter and J. D. Walecka, Quantum Theory of Many Particle Systems (Mc-Graw Hill, New York, 1971) p. 26, 45-47.

[16] K. Langanke, J.A. Maruhn and S.E. Koonin, Computational Nuclear Physics, (Springer-Verlag, Berlin, 1993).

[17] W. Nörenberg, G. Papp and P. Rozmej, Eur. Phys. J. **A 9**, 327 (2000).

[18] B. Jacquot, M. Colonna, S. Ayik and Ph. Chomaz, Nucl. Phys. **A 617**, 356 (1997).

APPENDIX A

DERIVATION OF DISPERSION RELATION

Momentum space matrix elements in Eq. 2.6 can be obtained as

$$< \boldsymbol{p}_1 \mid i\hbar \frac{\partial \delta\hat{\rho}(t)}{\partial t} \mid \boldsymbol{p}_2 >= i\hbar \frac{\partial}{\partial t} < \boldsymbol{p}_1 \mid \delta\hat{\rho}(t) \mid \boldsymbol{p}_2 > \tag{A.1}$$

$$\begin{aligned} < \boldsymbol{p}_1 \mid \left[\hat{h}_0, \delta\hat{\rho}_0\right] \mid \boldsymbol{p}_2 > &=< \boldsymbol{p}_1 \mid \hat{h}_0 \delta\hat{\rho}_0 \mid \boldsymbol{p}_2 > - < \boldsymbol{p}_1 \mid \delta\hat{\rho}_0 \hat{h}_0 \mid \boldsymbol{p}_2 > \\ &= \varepsilon_{\boldsymbol{p}_1} < \boldsymbol{p}_1 \mid \delta\hat{\rho}_0 \mid \boldsymbol{p}_2 > - < \boldsymbol{p}_1 \mid \delta\hat{\rho}_0 \mid \boldsymbol{p}_2 > \varepsilon_{\boldsymbol{p}_2} \\ &= (\varepsilon_{\boldsymbol{p}_1} - \varepsilon_{\boldsymbol{p}_2}) < \boldsymbol{p}_1 \mid \delta\hat{\rho}_0 \mid \boldsymbol{p}_2 > \end{aligned} \tag{A.2}$$

$$\begin{aligned} < \boldsymbol{p}_1 \mid \left[\delta\hat{U}, \hat{\rho}_0\right] \mid \boldsymbol{p}_2 > &=< \boldsymbol{p}_1 \mid \delta\hat{U}\hat{\rho}_0 \mid \boldsymbol{p}_2 > - < \boldsymbol{p}_1 \mid \hat{\rho}_0 \delta\hat{U} \mid \boldsymbol{p}_2 > \\ &=< \boldsymbol{p}_1 \mid \delta\hat{U} (\int d\boldsymbol{p}_2 \mid \boldsymbol{p}_2 >< \boldsymbol{p}_2 \mid) \hat{\rho}_0 \mid \boldsymbol{p}_2 \\ &\quad - < \boldsymbol{p}_1 \mid \hat{\rho}_0 (\int d\boldsymbol{p}_2 \mid \boldsymbol{p}_2 >< \boldsymbol{p}_2 \mid) \delta\hat{U} \mid \boldsymbol{p}_2 > \\ &= \int < \boldsymbol{p}_1 \mid \delta\hat{U} \mid \boldsymbol{p}_2 >< \boldsymbol{p}_2 \mid \hat{\rho}_0 \mid \boldsymbol{p}_2 > d\boldsymbol{p}_2 \\ &\quad - \int < \boldsymbol{p}_1 \mid \hat{\rho}_0 \mid \boldsymbol{p}_1 >< \boldsymbol{p}_1 \mid \delta\hat{U} \mid \boldsymbol{p}_2 > d\boldsymbol{p}_1 \\ &=< \boldsymbol{p}_1 \mid \delta\hat{U} \mid \boldsymbol{p}_2 > \rho_0(\boldsymbol{p}_2) - \rho_0(\boldsymbol{p}_1) < \boldsymbol{p}_1 \mid \delta\hat{U} \mid \boldsymbol{p}_2 > \\ &= \left[\rho_0(\boldsymbol{p}_2) - \rho_0(\boldsymbol{p}_1)\right] < \boldsymbol{p}_1 \mid \delta\hat{U} \mid \boldsymbol{p}_2 > \quad . \end{aligned} \tag{A.3}$$

After the combination of the terms, Eq. 2.5 becomes

$$i\hbar\frac{\partial}{\partial t}<\boldsymbol{p}_1|\delta\hat{\rho}(t)|\boldsymbol{p}_2>-(\varepsilon_{\boldsymbol{p}_1}-\varepsilon_{\boldsymbol{p}_2})<\boldsymbol{p}_1|\delta\hat{\rho}(t)|\boldsymbol{p}_2>$$

$$=\left[\rho_0(\boldsymbol{p}_2)-\rho_0(\boldsymbol{p}_1)\right]<\boldsymbol{p}_1|\delta\hat{U}|\boldsymbol{p}_2>. \quad \text{(A.4)}$$

Fourier transform with respect to time gives

$$\int i\hbar\frac{\partial}{\partial t}<\boldsymbol{p}_1|\delta\hat{\rho}(t)|\boldsymbol{p}_2>e^{i\omega t}dt-\int e^{i\omega t}(\varepsilon_{\boldsymbol{p}_1}-\varepsilon_{\boldsymbol{p}_2})<\boldsymbol{p}_1|\delta\hat{\rho}(t)|\boldsymbol{p}_2>dt$$

$$=\int e^{i\omega t}\left[\rho_0(\boldsymbol{p}_2)-\rho_0(\boldsymbol{p}_1)\right]<\boldsymbol{p}_1|\delta\hat{U}|\boldsymbol{p}_2>dt\,, \quad \text{(A.5)}$$

and finally

$$(\hbar\omega-\varepsilon_{\boldsymbol{p}_1}+\varepsilon_{\boldsymbol{p}_2})\int e^{i\omega t}<\boldsymbol{p}_1|\delta\hat{\rho}(t)|\boldsymbol{p}_2>dt$$

$$=\left[\rho_0(\boldsymbol{p}_2)-\rho_0(\boldsymbol{p}_1)\right]\int e^{i\omega t}<\boldsymbol{p}_1|\delta\hat{U}(t)|\boldsymbol{p}_2>dt\,. \quad \text{(A.6)}$$

APPENDIX B

FOURIER TRANSFORMATIONS

In order to evaluate the Fourier transform of the fluctuating part of the density matrix and the mean-field potential, we use the position space and momentum space representations in which we have the relations

$$< \boldsymbol{r} \mid \boldsymbol{p} >= e^{(i/\hbar)\boldsymbol{p}\cdot\boldsymbol{r}} \ , \tag{B.1}$$

$$< \boldsymbol{p} + \frac{\hbar\boldsymbol{k}}{2} \mid \boldsymbol{r} >= e^{-(i/\hbar)(\boldsymbol{p}+\hbar\boldsymbol{k}/2)\cdot\boldsymbol{r}} \ , \tag{B.2}$$

and

$$< \boldsymbol{r}' \mid \boldsymbol{p} - \frac{\hbar\boldsymbol{k}}{2} >= e^{(i/\hbar)(\boldsymbol{p}-\hbar\boldsymbol{k}/2)\cdot\boldsymbol{r}'} \ . \tag{B.3}$$

B.1. Fourier Transform of the fluctuating part of the density matrix

By Fourier transforming with respect to time, from Eq. 2.8.a, we obtain

$$\delta\rho(\boldsymbol{p} + \frac{\hbar\boldsymbol{k}}{2}, \boldsymbol{p} - \frac{\hbar\boldsymbol{k}}{2}; \omega) = \int e^{i\omega t} < \boldsymbol{p} + \frac{\hbar\boldsymbol{k}}{2} \mid \delta\hat{\rho} \mid \boldsymbol{p} - \frac{\hbar\boldsymbol{k}}{2} > dt$$

$$= \int e^{i\omega t} < \boldsymbol{p} + \frac{\hbar\boldsymbol{k}}{2} \mid \delta\hat{\rho} \mid \boldsymbol{p} - \frac{\hbar\boldsymbol{k}}{2} > dt$$

$$= \int e^{i\omega t} dt \int d\boldsymbol{r} d\boldsymbol{r}' < \boldsymbol{p} + \frac{\hbar\boldsymbol{k}}{2} \mid \boldsymbol{r} >< \boldsymbol{r} \mid \delta\hat{\rho} \mid \boldsymbol{r}' >< \boldsymbol{r}' \mid \boldsymbol{p} - \frac{\hbar\boldsymbol{k}}{2} >$$

$$= \int e^{i\omega t} dt \int d\boldsymbol{r} d\boldsymbol{r}' e^{-(i/\hbar)(\boldsymbol{p}+\hbar\boldsymbol{k}/2)\cdot\boldsymbol{r}} < \boldsymbol{r} \mid \delta\hat{\rho} \mid \boldsymbol{r}' > e^{(i/\hbar)(\boldsymbol{p}-\hbar\boldsymbol{k}/2)\cdot\boldsymbol{r}'} \ .$$

Then, integration over $\boldsymbol{p}$ gives

$$\int d\boldsymbol{p}\delta\rho(\boldsymbol{p}+\frac{\hbar\boldsymbol{k}}{2},\boldsymbol{p}-\frac{\hbar\boldsymbol{k}}{2};\omega)$$

$$=\int e^{i\omega t}dt\int d\boldsymbol{r}d\boldsymbol{r}'\int d\boldsymbol{p}e^{-(i/\hbar)\boldsymbol{p}\cdot(\boldsymbol{r}-\boldsymbol{r}')}e^{-(i/2)\boldsymbol{k}\cdot(\boldsymbol{r}+\boldsymbol{r}')}<\boldsymbol{r}\mid\delta\hat{\rho}\mid\boldsymbol{r}'>$$

$$=\int e^{i\omega t}dt\int d\boldsymbol{r}d\boldsymbol{r}'(2\pi\hbar)^3\delta(\boldsymbol{r}-\boldsymbol{r}')e^{-(i/2)\boldsymbol{k}\cdot(\boldsymbol{r}+\boldsymbol{r}')}<\boldsymbol{r}\mid\delta\hat{\rho}\mid\boldsymbol{r}'>$$

$$=\int e^{i\omega t}dt\int d\boldsymbol{r}(2\pi\hbar)^3e^{-i\boldsymbol{k}.\boldsymbol{r}}<\boldsymbol{r}\mid\delta\hat{\rho}\mid\boldsymbol{r}>$$

$$=(2\pi\hbar)^3\int e^{i\omega t}dt\int d\boldsymbol{r}e^{-i\boldsymbol{k}.\boldsymbol{r}}\delta n(\boldsymbol{r},t)$$

$$=(2\pi\hbar)^3\delta n(\boldsymbol{k},\omega)\ . \qquad \text{(B.4)}$$

B.2. Fourier Transform of the fluctuating part of the mean field matrix

By Fourier transforming with respect to time, from Eq. 2.8.b, it follows

$$\delta U(\boldsymbol{p}+\frac{\hbar\boldsymbol{k}}{2},\boldsymbol{p}-\frac{\hbar\boldsymbol{k}}{2};\omega)=\int e^{i\omega t}<\boldsymbol{p}+\frac{\hbar\boldsymbol{k}}{2}\mid\delta\hat{U}\mid\boldsymbol{p}-\frac{\hbar\boldsymbol{k}}{2}>dt$$

$$=\int e^{i\omega t}dt\int d\boldsymbol{r}d\boldsymbol{r}'<\boldsymbol{p}+\frac{\hbar\boldsymbol{k}}{2}\mid\boldsymbol{r}><\boldsymbol{r}\mid\left(\frac{\partial\hat{U}}{\partial\rho}\right)_0\delta\hat{\rho}\mid\boldsymbol{r}'><\boldsymbol{r}'\mid\boldsymbol{p}-\frac{\hbar\boldsymbol{k}}{2}>$$

$$=\int e^{i\omega t}dt\int d\boldsymbol{r}d\boldsymbol{r}'e^{-(i/\hbar)(\boldsymbol{p}+\hbar\boldsymbol{k}/2)\cdot\boldsymbol{r}}<\boldsymbol{r}\mid\left(\frac{\partial\hat{U}}{\partial\rho}\right)_0\delta\hat{\rho}\mid\boldsymbol{r}'>\ e^{(i/\hbar)(\boldsymbol{p}-\hbar\boldsymbol{k}/2)\cdot\boldsymbol{r}'}$$

$$=\int e^{i\omega t}dt\int d\boldsymbol{r}d\boldsymbol{r}'e^{-(i/\hbar)\boldsymbol{p}\cdot(\boldsymbol{r}-\boldsymbol{r}')}e^{-(i/2)\boldsymbol{k}\cdot(\boldsymbol{r}+\boldsymbol{r}')}\frac{\partial U}{\partial n}\delta n(\boldsymbol{r}',t)\delta(\boldsymbol{r}-\boldsymbol{r}')$$

$$=\int e^{i\omega t}dt\int d\boldsymbol{r}e^{-i\boldsymbol{k}\cdot\boldsymbol{r}}\frac{\partial U(\boldsymbol{r})}{\partial n}\delta n(\boldsymbol{r},t)$$

$$=\frac{\partial U(\boldsymbol{k})}{\partial n}\delta n(\boldsymbol{k},\omega)\ . \qquad \text{(B.5)}$$

By writing the momenta in Eq. 2.7 as $\boldsymbol{p}_1 = \boldsymbol{p} + \frac{\hbar \boldsymbol{k}}{2}$, $\boldsymbol{p}_2 = \boldsymbol{p} - \frac{\hbar \boldsymbol{k}}{2}$, we obtain

$$(\hbar\omega_k - \varepsilon_{\boldsymbol{p}+\hbar\boldsymbol{k}/2} + \varepsilon_{\boldsymbol{p}-\hbar\boldsymbol{k}/2})\delta\rho(\boldsymbol{p}+\hbar\boldsymbol{k}/2, \boldsymbol{p}-\hbar\boldsymbol{k}/2;\omega)$$

$$= \left[\rho_0(\boldsymbol{p}-\hbar\boldsymbol{k}/2) - \rho_0(\boldsymbol{p}+\hbar\boldsymbol{k}/2)\right]\delta U(\boldsymbol{p}+\hbar\boldsymbol{k}/2, \boldsymbol{p}-\hbar\boldsymbol{k}/2;\omega) \ , \quad \text{(B.6)}$$

and integrating over $\boldsymbol{p}$ results in

$$\int \frac{d\boldsymbol{p}}{(2\pi\hbar)^3}\delta\rho(\boldsymbol{p}+\hbar\boldsymbol{k}/2, \boldsymbol{p}-\hbar\boldsymbol{k}/2;\omega)$$

$$= \int \frac{d\boldsymbol{p}}{(2\pi\hbar)^3}\frac{\partial U(\boldsymbol{k})}{\partial n}\delta n(\boldsymbol{k},\omega)\frac{\left[\rho_0(\boldsymbol{p}-\hbar\boldsymbol{k}/2) - \rho_0(\boldsymbol{p}+\hbar\boldsymbol{k}/2)\right]}{(\hbar\omega_k - \varepsilon_{\boldsymbol{p}+\hbar\boldsymbol{k}/2} + \varepsilon_{\boldsymbol{p}-\hbar\boldsymbol{k}/2})} \ . \quad \text{(B.7)}$$

From Eq. 2.10 it then follows that

$$\frac{\delta n(\boldsymbol{k},\omega)}{\delta n(\boldsymbol{k},\omega)} = \frac{\partial U(\boldsymbol{k})}{\partial n}\int \frac{d\boldsymbol{p}}{(2\pi\hbar)^3}\frac{\left[\rho_0(\boldsymbol{p}-\hbar\boldsymbol{k}/2) - \rho_0(\boldsymbol{p}+\hbar\boldsymbol{k}/2)\right]}{(\hbar\omega_k - \varepsilon_{\boldsymbol{p}+\hbar\boldsymbol{k}/2} + \varepsilon_{\boldsymbol{p}-\hbar\boldsymbol{k}/2})} \ .$$

Therefore, Eq. 2.7 becomes

$$1 = \frac{\partial U(\boldsymbol{k})}{\partial n}\int \frac{d\boldsymbol{p}}{(2\pi\hbar)^3}\frac{\rho_0(\boldsymbol{p}-\hbar\boldsymbol{k}/2) - \rho_0(\boldsymbol{p}+\hbar\boldsymbol{k}/2)}{(\hbar\omega_k - \varepsilon_{\boldsymbol{p}+\hbar\boldsymbol{k}/2} + \varepsilon_{\boldsymbol{p}-\hbar\boldsymbol{k}/2})} \ . \quad \text{(2.15)}$$

This is the quantal dispersion relation for the frequency of the collective mode corresponding to the wave number $\boldsymbol{k}$.

APPENDIX C

EVALUATION OF THE INTEGRAL IN THE DISPERSION RELATION

C.1. Dispersion Relation at Zero Temperature

In order to evaluate the integral in the dispersion relation at $T = 0$, we note that with Eq. 3.3 and Eq. 3.4 the integrand in Eq. 2.11 becomes

$$\frac{\theta(p_F - |\boldsymbol{p} - \hbar\boldsymbol{k}/2|) - \theta(p_F - |\boldsymbol{p} + \hbar\boldsymbol{k}/2|)}{\hbar\omega_k - (\boldsymbol{p} + \hbar\boldsymbol{k}/2)^2/2m + (\boldsymbol{p} - \hbar\boldsymbol{k}/2)^2/2m}$$

$$= \frac{\theta(p_F - |\boldsymbol{p} - \hbar\boldsymbol{k}/2|)}{\hbar\omega_k - \hbar\boldsymbol{k}.\boldsymbol{p}/m} - \frac{\theta(p_F - |\boldsymbol{p} + \hbar\boldsymbol{k}/2|)}{\hbar\omega_k - \hbar\boldsymbol{k}.\boldsymbol{p}/m} \quad . \quad \text{(C.1)}$$

We integrate Eq. C.1 term by term as

$$\int d\boldsymbol{p} \frac{\theta(p_F - |\boldsymbol{p} - \hbar\boldsymbol{k}/2|)}{\hbar\omega_k - \hbar\boldsymbol{k}.\boldsymbol{p}/m} = A \ ,$$

$$\int d\boldsymbol{p} \frac{\theta(p_F - |\boldsymbol{p} + \hbar\boldsymbol{k}/2|)}{\hbar\omega_k - \hbar\boldsymbol{k}.\boldsymbol{p}/m} = B \ .$$

For the evaluation of the term A we make the transformation $\boldsymbol{p} - \hbar\boldsymbol{k}/2 \rightarrow \boldsymbol{p}$ and we obtain

$$A = \int d\boldsymbol{p} \frac{\theta(p_F - p)}{\hbar\omega_k - \hbar\boldsymbol{k}.(\boldsymbol{p} + \hbar\boldsymbol{k}/2)/m} = \int d\boldsymbol{p} \frac{\theta(p_F - p)}{\hbar\omega_k - \hbar\boldsymbol{k}.\boldsymbol{p}/m - \hbar^2 k^2/2m} \ .$$

Measuring all momentum vectors in terms of p_F ($p/p_F \to p$), we obtain

$$A = \int p_F^3 d\boldsymbol{p} \frac{\theta(1-p)}{p_F(\hbar\omega_k / p_F - \hbar k p\cos\theta / m - \hbar^2 k^2 / 2mp_F)}$$
$$= \int p_F^2 d\boldsymbol{p} \frac{m}{\hbar k} \frac{\theta(1-p)}{(m\omega_k / kp_F - p\cos\theta - \hbar k / 2p_F)}$$
$$= \int p_F^2 d\boldsymbol{p} \frac{m}{\hbar k} \frac{\theta(1-p)}{(s - p\cos\theta - s_0)} \ . \qquad \text{(C.2.a)}$$

For the evaluation of the term B we make the transformation $\boldsymbol{p} + \hbar\boldsymbol{k}/2 \to \boldsymbol{p}$ which results in

$$B = \int p_F^3 d\boldsymbol{p} \frac{\theta(1-p)}{p_F(\hbar\omega_k / p_F - \hbar k p\cos\theta / m + \hbar^2 k^2 / 2mp_F)}$$
$$= \int p_F^2 d\boldsymbol{p} \frac{m}{\hbar k} \frac{\theta(1-p)}{(m\omega_k / kp_F - p\cos\theta + \hbar k / 2p_F)}$$
$$= \int p_F^2 d\boldsymbol{p} \frac{m}{\hbar k} \frac{\theta(1-p)}{(s - p\cos\theta + s_0)} \ , \qquad \text{(C.2.b)}$$

where $s = m\omega_k / kp_F$ and $s_0 = \hbar k / 2p_F$ are introduced as dimensionless variables. Combining our results gives us the final expression as

$$A - B = {p_F}^2 \frac{m}{\hbar k} \int d\boldsymbol{p}\theta(1-p)\left[\frac{1}{(s - p\cos\theta - s_0)} - \frac{1}{(s - p\cos\theta + s_0)}\right] , \qquad \text{(C.3)}$$

$$A - B = 2\pi 2p_F m\left\{-\frac{1}{2} + \frac{1}{8s_0}\left[(s+s_0)^2 - 1\right] \ln\frac{s+s_0+1}{s+s_0-1}\right.$$
$$\left. - \frac{1}{8s_0}\left[(s-s_0)^2 - 1\right] \ln\frac{s-s_0+1}{s-s_0-1}\right\} \ . \qquad \text{(C.4)}$$

C.1.1. Classical Limit

In order to evaluate $\hbar \to 0$ limit of the zero temperature dispersion relation, we start with Eq. 3.7

$$\frac{1}{F_0(k)} + \frac{1}{2}$$

$$= \frac{1}{8}\left[(\frac{s^2}{s_0} + 2s + s_0 - 1) \ \ln\frac{s + s_0 + 1}{s + s_0 - 1} - (\frac{s^2}{s_0} - 2s + s_0 - 1) \ \ln\frac{s - s_0 + 1}{s - s_0 - 1}\right]$$

$$= \frac{1}{8}\Big[\ \frac{s^2 - 1}{s_0}\ln(\frac{s + s_0 + 1}{s + s_0 - 1}\frac{s - s_0 - 1}{s - s_0 + 1}) + 2s\ln(\frac{s + s_0 + 1}{s + s_0 - 1}\frac{s - s_0 + 1}{s - s_0 - 1})$$

$$+ s_0 \ln(\frac{s + s_0 + 1}{s + s_0 - 1}\frac{s - s_0 - 1}{s - s_0 + 1}) \ \Big] .$$

In the limit of $s_0 \to 0$ the third term goes to zero and we obtain

$$\frac{1}{F_0(k)} + \frac{1}{2} = \frac{1}{8}\left[\frac{s^2 - 1}{s_0}\ln(\frac{s + s_0 + 1}{s + s_0 - 1}\frac{s - s_0 - 1}{s - s_0 + 1}) + 4s\ln(\frac{s + 1}{s - 1})\right] \qquad \text{(C.5)}$$

which is indeterminate. Applying L'Hospital's Rule to the indeterminate term, the limit can be evaluated as

$$\lim_{s_0 \to 0}\left[\frac{s^2 - 1}{s_0}\ln(\frac{s + s_0 + 1}{s + s_0 - 1}\frac{s - s_0 - 1}{s - s_0 + 1})\right] = (s^2 - 1)\frac{-4}{s^2 - 1} = -4 \ , \qquad \text{(C.6)}$$

and Eq C.5 becomes

$$\frac{1}{F_0(k)} + 1 = \frac{s}{2}\ln(\frac{s + 1}{s - 1}) \ . \qquad \text{(C.7)}$$

C.2. Dispersion Relation at Finite Temperature

For the evaluation of the integral in the dispersion relation at finite temperature we use the transformation $\boldsymbol{p} - \hbar\boldsymbol{k}/2 \to \boldsymbol{p}$

$$I = \int \frac{d\boldsymbol{p}}{(2\pi\hbar)^3}\left(\frac{\rho_0(\boldsymbol{p})}{i\hbar/\tau_k - \varepsilon(\boldsymbol{p}+\hbar\boldsymbol{k}) + \varepsilon(\boldsymbol{p})} - \frac{\rho_0(\boldsymbol{p}+\hbar\boldsymbol{k})}{i\hbar/\tau_k - \varepsilon(\boldsymbol{p}+\hbar\boldsymbol{k}) + \varepsilon(\boldsymbol{p})}\right). \qquad \text{(C.8)}$$

We can integrate Eq. C.8 term by term as

$$I = \int \frac{d\boldsymbol{p}}{(2\pi\hbar)^3}\frac{\rho_0(\boldsymbol{p})}{i\hbar/\tau_k - \varepsilon(\boldsymbol{p}+\hbar\boldsymbol{k}) + \varepsilon(\boldsymbol{p})} - \int \frac{d\boldsymbol{p}}{(2\pi\hbar)^3}\frac{\rho_0(\boldsymbol{p}+\hbar\boldsymbol{k})}{i\hbar/\tau_k - \varepsilon(\boldsymbol{p}+\hbar\boldsymbol{k}) + \varepsilon(\boldsymbol{p})}\,. \qquad \text{(C.9)}$$

With the transformation $\boldsymbol{p} + \hbar\boldsymbol{k} \to -\boldsymbol{p}$ in the second term, we obtain

$$I = \int \frac{d\boldsymbol{p}}{(2\pi\hbar)^3}\frac{\rho_0(\boldsymbol{p})}{i\hbar/\tau_k - \varepsilon(\boldsymbol{p}+\hbar\boldsymbol{k}) + \varepsilon(\boldsymbol{p})} - \int \frac{d\boldsymbol{p}}{(2\pi\hbar)^3}\frac{\rho_0(\boldsymbol{p})}{i\hbar/\tau_k - \varepsilon(\boldsymbol{p}) + \varepsilon(\boldsymbol{p}+\hbar\boldsymbol{k})}, \qquad \text{(C.10)}$$

since $\rho_0(\boldsymbol{p}) \equiv \rho_0(-\boldsymbol{p})$ and $\varepsilon(\boldsymbol{p}) \equiv \varepsilon(-\boldsymbol{p})$. If we write the energy terms explicitly Eq. C.10 becomes

$$I = \int \frac{d\boldsymbol{p}}{(2\pi\hbar)^3}\rho_0(\boldsymbol{p})\frac{2\ (2\hbar\boldsymbol{p}.\boldsymbol{k}/2m + \hbar^2k^2/2m)}{-(\hbar/\tau_k)^2 - (2\hbar\boldsymbol{p}.\boldsymbol{k}/2m + \hbar^2k^2/2m)^2}. \qquad \text{(C.11)}$$

The explicit form of the dot product gives rise to the angular terms in the integrand and the integral becomes

$$I = \int \frac{d\boldsymbol{p}}{(2\pi\hbar)^3}\rho_0(\boldsymbol{p})\frac{2\ (2\hbar pk\cos\theta/2m + \hbar^2k^2/2m)}{-(\hbar/\tau_k)^2 - (2\hbar pk\cos\theta/2m + \hbar^2k^2/2m)^2}\,. \qquad \text{(C.12)}$$

The angular part of this integral can be evaluated by using the spherical coordinates

$$I = \int_0^{2\pi} d\varphi \int_0^{\pi} d\theta \int \frac{p^2 \sin\theta dp}{(2\pi\hbar)^3} \rho_0(p) \frac{2\ (2\hbar pk\cos\theta / 2m + \hbar^2 k^2 / 2m)}{-(\hbar/\tau_k)^2 - (2\hbar pk\cos\theta / 2m + \hbar^2 k^2 / 2m)^2} \quad , \text{(C.13)}$$

and the result is found to be as

$$I = 2\pi \int \frac{dp}{(2\pi\hbar)^3} \rho_0(p) p \frac{2m}{2\hbar k} \{\ln|(\hbar/\tau_k)^2 + (-2\hbar pk / 2m + \hbar^2 k^2 / 2m)^2| - \ln|(\hbar/\tau_k)^2 + (2\hbar pk / 2m + \hbar^2 k^2 / 2m)^2|\}. \quad \text{(C.14)}$$

APPENDIX D

FERMI WAVE NUMBER AND FERMI ENERGY

For a uniform Fermi gas, the expectation value of the number operator in the normalized ground state $|F\rangle$ is [15]

$$N = \langle F|\hat{N}|F\rangle = \sum_{k\lambda}\langle F|\hat{n}_{k\lambda}|F\rangle = \sum_{k\lambda}\theta(k_F - k) \qquad \text{(C.15)}$$

where $\hat{n}_{k\lambda}$ is the number-density operator.

Since the Pauli exclusion principle allows only two fermions in each momentum eigenstate, one with spin-up and one with spin-down, the normalized ground state $|F\rangle$ is obtained by filling the momentum states up to a value, the Fermi momentum $p_F = \hbar k_F$, and we have a spin degeneracy factor of 2 for protons and 2 for neutrons. In the limit that volume of the system becomes infinite, we can replace sums over states by integrals [15] as

$$N = \sum_{\lambda_p=1}^{2}\sum_{\lambda_n=1}^{2}\frac{V}{(2\pi)^3}\int\theta(k_F - k)d^3k = \frac{4V}{(2\pi)^3}4\pi\int_0^{k_F}k^2dk = \frac{2V}{3\pi^2}k_F^3 \ . \qquad \text{(C.16)}$$

Then the maximum wave number k_F is found to be

$$k_F = \left(\frac{3\pi^2 N}{2V} \right)^{1/3} = \left(\frac{3\pi^2 n_0}{2} \right)^{1/3}, \tag{C.17}$$

where n_0 is the local density and energy of the Fermi level is

$$\varepsilon_F = \frac{\hbar^2 k_F^2}{2m} = \frac{\hbar^2}{2m} \left(\frac{3\pi^2 n_0}{2} \right)^{2/3}. \tag{C.18}$$